OXFORD

Cerebral Cortex, August 2019; 3319–3330

doi: 10.1093/cercor/bhy201
Advance Access Publication Date: 23 August 2018
Original Article

ORIGINAL ARTICLE

Atypical Local and Distal Patterns of Occipito-frontal Functional Connectivity are Related to Symptom Severity in Autism

R. Joanne Jao Keehn[1], Sangeeta Nair[1,2], Ellyn B. Pueschel[1], Annika C. Linke[1], Inna Fishman[1,3] and Ralph-Axel Müller[1,3]

[1]Brain Development Imaging Laboratory, Department of Psychology, San Diego State University, San Diego, CA, USA, [2]Department of Psychology, University of Alabama, at Birmingham, Birmingham, AL, USA and [3]Joint Doctoral Program in Clinical Psychology, San Diego State University and University of California, San Diego, San Diego, CA, USA

Address correspondence to R. Joanne Jao Keehn, Department of Psychology, San Diego State University, 6363 Alvarado Ct., Suite 200, San Diego, CA 92120, USA. Email: rjao@sdsu.edu

Abstract

Autism spectrum disorders (ASDs) are increasingly prevalent neurodevelopmental disorders characterized by sociocommunicative impairments. Growing consensus indicates that neurobehavioral abnormalities require explanation in terms of interconnected networks. Despite theoretical speculations about increased local and reduced distal connectivity, links between local and distal functional connectivity have not been systematically investigated in ASDs. Specifically, it remains open whether hypothesized local overconnectivity may reflect isolated versus overly integrative processing. Resting state functional MRI data from 57 children and adolescents with ASDs and 51 typically developing (TD) participants were included. In regional homogeneity (ReHo) analyses, pericalcarine visual cortex was found be locally overconnected (ASD > TD). Using this region as seed in whole-brain analyses, we observed overconnectivity in distal regions, specifically middle frontal gyri, for an ASD subgroup identified through *k*-means clustering. While in this subgroup local occipital to distal frontal overconnectivity was associated with greater symptom severity, a second subgroup showed the opposite pattern of connectivity and symptom severity correlations. Our findings suggest that increased local connectivity in ASDs is region-specific and may be partially associated with more integrative long-distance connectivity. Results also highlight the need to test for subtypes, as differential patterns of brain–behavior links were observed in two distinct subgroups of our ASD cohort.

Key words: autism, frontal cortex, functional connectivity MRI, local connectivity, visual cortex

Introduction

Autism spectrum disorders (ASDs) are an increasingly prevalent set of neurodevelopmental disorders (CDC 2015), characterized by sociocommunicative impairments and repetitive behaviors (American Psychiatric Association 2013). A neurobiological basis of ASDs has been recognized for many decades (Damasio and Maurer 1978), but anatomical and functional brain findings have been highly diverse. Due to the complexity of the disorder and heterogeneity in symptoms, attempts to explain autism with respect to strictly localized brain anomalies have not been successful. Instead, there has been a growing consensus that behavioral and brain abnormalities can only be explained at the level of interconnected networks (Menon 2011; Vissers et al. 2012).

Efficient functioning of specialized sensorimotor and cognitive networks relies on two complementary organizing principles: functional segregation (or differentiation), emphasizing

the degree to which different regions or networks are specialized, and functional integration, referring to the communication between regions within a specialized network (Johnson 2011; Sporns 2013; Maximo et al. 2014). Functional differentiation at the local level, and the balance between segregation and integration support the emergence of efficient and specialized networks in neurotypical development (Johnson 2011).

One method for mapping large-scale functional networks that span distributed areas is functional connectivity MRI (fcMRI), which detects interregional temporal correlations of the blood oxygen level-dependent (BOLD) signal (Van Dijk et al. 2010; Buckner et al. 2013). In a task-free condition, spontaneous low-frequency time series fluctuations are thought to reflect synchronized neuronal activity (Birn 2007), interpreted as intrinsic functional connectivity (iFC). A growing number of studies has examined iFC using resting state (rs) fMRI. While there have been numerous reports of atypical distal connectivity in ASDs (Vissers et al. 2012), findings are mixed regarding over- versus underconnectivity (e.g., Supekar et al. 2013; Di Martino et al. 2014; Nair et al. 2014; Abbott et al. 2016).

Comparatively few studies have examined local connectivity in ASDs (Paakki et al. 2010; Shukla et al. 2010; Keown et al. 2013; Maximo et al. 2013; Itahashi et al. 2015; Jiang et al. 2015; Dajani and Uddin 2016), and results have been as divergent as for studies of distal connectivity. For example, whereas Di Martino et al. (2014) observed local overconnectivity in ASDs in right prefrontal cortex in a large multisite sample, such effects were detected in posterior visual cortices in smaller samples (Maximo et al. 2013), including subsets of the same multisite sample (Nair et al. 2017). Such atypically increased local synchrony of the BOLD signal may be an indicator of reduced differentiation (Shih et al. 2011; Nebel et al. 2014).

While the ASDs literature has generated numerous findings of atypical iFC – many for distal and some for local connectivity – the links between the two remain poorly understood. Although a hypothesis of local overconnectivity associated with long-range underconnectivity in ASDs proposed by Belmonte et al. (2004) has been frequently reiterated via cross-citation (e.g., Minshew and Williams 2007; Williams and Casanova 2010; Wass 2011; Vissers et al. 2012; Maximo et al. 2014), there has been surprisingly little systematic research on the links between local and distal connectivity in ASDs. One related study by Shih et al. (2011) found that reduced differentiation within posterior superior temporal sulcus (equivalent to greater synchrony of BOLD fluctuations across adjacent subregions) was associated with diffuse distal overconnectivity in children and adolescents with ASDs, which is inconsistent with the "Belmonte hypothesis."

In the present study, we investigated links between local and distal iFC in ASDs. The regional homogeneity (ReHo) approach (Zang et al. 2004) was used to examine whether atypically increased (or reduced) local connectivity is related to isolated processing (associated with distal underconnectivity) or, conversely, overly integrative processing (associated with distal overconnectivity). Additionally, we investigated whether links between local and distal iFC are associated with symptomatology in autism.

Materials and Methods

Participants

The current study included 57 high-functioning children and adolescents with ASDs and 51 typically developing (TD) control participants between 8 and 18 years of age. Diagnoses in the ASD group were established using the Autism Diagnostic Interview-Revised (ADI-R; Lord et al. 1994), the Autism Diagnostic Observation Schedule (ADOS; Lord et al. 2000), and expert clinical decision according to DSM-5 (American Psychiatric Association 2013). Three ASD participants fulfilled criteria (one for autistic disorder, two for Asperger's Syndrome) on the DSM-IV (American Psychiatric Association 2000), but not the DSM-5, due to the higher threshold for the repetitive and restrictive diagnostic criteria on the DSM-5. Children with autism-related medical conditions (e.g., Fragile-X syndrome, tuberous sclerosis) or other neurological conditions (e.g., epilepsy, Tourette's Syndrome) were excluded. TD participants had no reported history of ASDs or any other neurological or psychiatric condition. Groups were matched on gender, handedness, age, IQ, and in-scanner head motion (Table 1). All participants scored above the cutoff for intellectual disability (IQ > 70) on the Wechsler Abbreviated Scale of Intelligence–2nd ed. (WASI-2; Wechsler 1999). Hand preference

Table 1 Demographic and diagnostic information

	TD (n = 51)		ASD (n = 57)		Group comparison
	Mean (SD)	Range	Mean (SD)	Range	
Gender	9 female		10 female		$\chi^2(1) < .001$, P = 0.99
Handedness	8 left		9 left		$\chi^2(1) < .001$, P = 0.99
Age in years	13.2 (2.7)	8.0–17.6	13.8 (2.6)	9.0–18.0	$t(106) = 1.1$, P = 0.29
Verbal IQ	106.9 (9.9)	78–127	102.0 (17.3)	70–147	$t(106) = -1.8$, P = 0.08
Non-verbal IQ	105.1 (12.7)	62–129	106.6 (18.7)	53–145	$t(106) = 0.5$, P = 0.63
Full-Scale IQ	106.4 (10.7)	79–126	104.4 (17.2)	66–141	$t(106) = -0.7$, P = 0.46
RMSD	0.06 (0.03)	0.02–0.14	0.06 (0.03)	0.02–0.11	$t(106) = -0.1$, P = 0.93
ADOS[a]					
Social interaction	–	–	7.6 (2.7)	2–14	–
Communication	–	–	3.9 (2.1)	0–13	–
Repetitive/Restricted	–	–	2.2 (1.5)	0–5	–
ADI-R[b]					
Social interaction	–	–	18.3 (5.0)	6–28	–
Communication	–	–	13.5 (5.0)	2–24	–
Repetitive behavior	–	–	6.1 (2.2)	1–12	–

[a]Subdomain data not available for 3 ASD participants.
[b]Subdomain data not available for 1 ASD participant.

was assessed using the Edinburgh Handedness Inventory (Oldfield 1971). The Institutional Review Boards of San Diego State University and University of California San Diego approved the experimental protocol, and informed consent and written assent were obtained for all participants.

Data Acquisition and Image Preprocessing

Resting-state imaging data were acquired on a GE 3T MR750 scanner with an 8-channel head coil at the University of California San Diego Center for Functional MRI. High-resolution structural images were acquired with a standard FSPGR T1-weighted sequence (TR: 8.136 ms; TE: 3.172 ms; flip angle: 8°; field of view [FOV]: 25.6 cm; matrix: 256 × 256; 172 slices; resolution: 1 mm^3). Resting-state functional T2*-weighted images were obtained using a single-shot gradient-recalled, echo-planar pulse sequence. One 6:10 min scan was acquired consisting of 185 whole-brain volumes (TR: 2000 ms; TE: 30 ms; slice thickness: 3.4 mm; flip angle: 90°; FOV: 22.0 cm; matrix: 64 × 64; in-plane resolution: 3.44 mm^2). The first five time points were discarded to allow for equilibration effects, leaving 180 time points for analysis. Participants were instructed: "Keep your eyes on the cross-hair, relax, let your mind wander, and try not to fall asleep." Eye status was monitored throughout the scan with an in-bore video camera to ensure that participants' eyes were open. Additionally, eye status (e.g., fixated, exploring, closed) was coded frame-by-frame in a subset of participants. Post-hoc analyses of the percentage of scan time for each eye status showed that both groups followed instructions similarly and predominantly fixated on the cross hair (ASD mean: 92.5%; TD mean: 83.4%), and two-sample *t*-tests showed no significant between-group differences (eyes fixated: $t(19) = 0.98$, $P = 0.34$; eyes exploring: $t(19) = -1.51$, $P = 0.15$; eyes closed: $t(19) = -0.73$, $P = 0.47$).

Functional images were processed using Analysis of Functional NeuroImages (AFNI; Cox 1996) and FMRI software library (FSL; Smith et al. 2004). Functional images were slice-time corrected to compensate for temporal offset between slice acquisitions, and motion corrected to align all acquired volumes. Images were field-map corrected to minimize effects of magnetic field inhomogeneity. Functional images were registered to the anatomical images via FSL's FLIRT (Jenkinson and Smith 2001), and structural images were normalized to the atlas space of the MNI152 template using FSL's nonlinear registration tool (FNIRT). The resulting transformation matrix was then used to spatially normalize the functional images, with both images resampled to 3 mm isotropic voxels. To isolate spontaneous low-frequency BOLD fluctuations (Cordes et al. 2001), fMRI time series were bandpass filtered ($0.008 < f < 0.08$ Hz), using a second-order Butterworth filter, which was also applied to all nuisance regressors described below. Differences in smoothness between individual datasets (resulting from motion correction and spatial normalization, for example) directly impact time series correlations between neighboring voxels and could confound local connectivity comparisons. We therefore set effective smoothness of all datasets to a Gaussian FWHM of 6 mm. Participant-level masks for cerebral white matter and lateral ventricles were created using FSL's FAST automated segmentation (Zhang et al. 2001), and an average time series for each was extracted. Time courses for white matter, ventricles, and 6 rigid-body motion parameters (from motion correction), each with their first derivatives, were used as nuisance regressors.

Given evidence suggesting that global signal regression (GSR) has the potential to distort between-group effects (Gotts et al. 2013; Abbott et al. 2016) and may impact ReHo (Qing et al. 2015), we performed primary analyses without regressing the global signal (i.e., the time series of the averaged whole brain signal), which likely reflects a combination of "true" (neuronal-activity based) signal fluctuations and noise (Fox et al. 2009; Schölvinck et al. 2010; Keller et al. 2013). Nevertheless, as GSR is a powerful noise-reduction tool in resting state fcMRI (Power et al. 2014), analyses were also performed with GSR using the 6 motion parameters, white matter, ventricles, global signal, and their first derivatives as regressors (Power et al. 2015). Results are described below and presented in the Supplementary Materials.

Head Motion

Due to the known impact of head motion on BOLD correlations (Power et al. 2012; van Dijk et al. 2012), several quality control measures were taken during data preprocessing and analysis to minimize head motion effects. Six rigid-body motion regressors and their derivatives were estimated, modeled, and used to censor time points with excessive head motion. Time points with head motion >0.5 mm, together with the two following time points, were censored. All participants included in the current study retained at least 80% of time points. Additionally, no participants with movements >0.1 mm over more than 5 consecutive time points were included. There were no group differences in the root mean squared displacement (RMSD; i.e., the root mean squared values of the detrended realignment; Table 1), suggesting that any detected connectivity differences were unlikely related to differences in motion.

Local Functional Connectivity Measure: Regional Homogeneity

Regional homogeneity (ReHo) uses Kendall's coefficient of concordance (KCC; Kendall and Gibbsons 1990), which relies on rank correlations to assess the homogeneity of a voxel and its neighboring voxels. KCC within a given cluster of voxels is equal to the parameter W (ranging from 0 to 1),

$$W = \frac{\sum (R_i)^2 - n(\bar{R})^2}{\frac{1}{12}K^2(n^3 - n)}$$

where R_i is the sum rank of the ith time point; $\bar{R}$ is the mean of the R_is; K is the number of time series within a selected cluster and n is the number of ranks, as determined by the number of time points (Zang et al. 2004).

Maximo et al. (2013) examined the effect of varying cluster sizes of 7, 19, and 27 voxels on ReHo, and found more modest between-group effects at finer spatial scales. For the present study, ReHo was therefore computed for a cluster size of 27 voxels and a gray-matter mask was used to reduce partial-volume effects. Individual-level ReHo maps were obtained and standardized into KCC (W) z'-values by subtracting the mean voxel-wise KCC (W) obtained for the entire whole-brain mask and then dividing by the standard deviation. The standardization of KCC (W) into z'-maps distributes whole-brain ReHo maps around zero and may aid in interpreting regionally specific differences in local connectivity. Group differences were then examined with two-sample *t*-tests. Randomization and permutation tests were implemented via the updated, bug-fixed 3dClustSim program called by the 3dttest++ function in AFNI to correct for multiple comparisons in order to obtain a corrected significance level of $P < 0.05$, with an uncorrected

significance level of $P < 0.005$ and a minimum cluster volume of 45 voxels (Eklund et al. 2016; Cox et al. 2017).

Whole-Brain fcMRI Analysis

Clusters of significant between-group ReHo effects were used as seeds for whole-brain fcMRI analyses. An average BOLD time series extracted from ReHo seeds in each participant was Pearson correlated with the time courses of every other brain voxel. Correlation coefficients were Fisher transformed to normally distributed z'-scores. Two-sample *t*-tests were conducted to examine between-group iFC effects, and a gray matter mask was applied to constrain results to gray matter. Statistical maps were set to an uncorrected threshold of $P < 0.01$; this rather liberal threshold was used to explore distal connectivity patterns.

Post-hoc Selection of Regions-of-Interest

Two additional regions-of-interests (ROIs) that were maximally distal to the ReHo seed were selected from the Harvard Oxford atlas (Desikan et al. 2006). The left frontal pole (1792 voxels) and right frontal pole (2110 voxels) were gray matter masked and included in subsequent ReHo seed to ROI fcMRI analyses (Fig. 1A).

Additionally, *k*-means clustering (10 000 iterations; tested values from $k = 1$ to $k = 6$) was performed on iFC patterns between the ReHo seed and frontal pole ROIs within the ASD group. The optimal number of clusters was determined by the silhouette criterion, using a squared Euclidean distance function. This clustering was implemented to examine ASD subgroupings on local and distal connectivity effects.

Correlational Analyses

Local (ReHo) and distal (ReHo seed to frontal pole) iFC (z') data were entered into correlational analyses with subdomains of the ADOS (Lord et al. 2000) and ADI-R (Lord et al. 1994) to examine the links between neural patterns and autism symptomatology overall. Age and head motion (RMSD) were included as covariates in these analyses.

Results

Local Connectivity (ReHo)

Direct group comparisons of ReHo patterns (with standardization, but without GSR) showed a single cluster of increased local connectivity in the ASD compared with the TD group with peak in primary visual cortex (V1; Fig. 1B, Table 2). This locally overconnected ReHo cluster (ASD > TD) was used as a seed in whole-brain functional connectivity analyses.

Whole-Brain Distal Connectivity

Results of the whole-brain iFC analysis for the locally overconnected V1 ReHo seed showed two overconnected clusters (ASD > TD) in distal frontal regions, specifically, middle frontal gyri (MFG; Fig. 1C, Table 2). While these findings did not survive stringent cluster correction, effect sizes were medium to large (left MFG cluster Cohen's $d = .71$; right MFG $d = .66$). In addition, two ROIs from the Harvard Oxford atlas that were maximally distal to the seed – left and right frontal pole (FP; Fig. 1A) – were selected. For these ROIs, BOLD correlations with the V1 seed were predominantly higher in the ASD than the TD group with a 2.9:1 ratio (left FP) and a 3.2:1 ratio (right FP) of voxel-wise over- versus underconnectivity (see Supplementary Fig. S1). ReHo (z') within the local overconnectivity cluster was not correlated with distal connectivity in the frontal ROIs in either group.

ASD Subgroupings

K-means clustering revealed two subsets of participants with ASD (optimal silhouette value = 0.49 for $k = 2$; Supplementary Fig. S2). Despite distinct connectivity profiles (Fig. 2A), the two subgroups showed overall little difference on demographic and diagnostic measures (Table 3).

For local connectivity (ReHo) within the V1 cluster, the ASD1 subgroup showed high KCC (*W*) values, significantly above those from the TD group and marginally above those from the ASD2 subgroup (Fig. 2B, Table 4). A 2 (distal region pairs: V1 – left MFG, V1 – right MFG) × 3 (group: ASD1, ASD2, TD) repeated measures Analysis of Variance (ANOVA) indicated a main effect of group ($F(2,105) = 15.85$, $P < 0.001$). Post-hoc two-sample *t*-tests at the group-level showed higher V1 distal connectivity (z') in the ASD1 subgroup compared with both the ASD2 subgroup and TD group, but no significant differences between the ASD2 subgroup and TD group (Fig. 2C, Table 4). A 3 (ROI pairs: V1 – left FP, V1 – right FP, left FP – right FP) × 3 (group: ASD1, ASD2, TD) repeated measures ANOVA further showed main effects of group ($F(2,105) = 29.81$, $P < 0.001$) and ROI pairing ($F(1.48,155.57) = 330.64$, $P < 0.001$, $MSe = 17.19$), with a marginal group by ROI pair interaction effect ($F(2.96,155.57) = 2.28$, $P = 0.082$, $MSe = 0.12$). Mauchly's test indicated that the assumption of sphericity of the main and interaction effects for ROI pairing had been violated ($\chi^2(2) = 44.79$, $P < 0001$); therefore, degrees of freedom were corrected using the Greenhouse-Geisser estimates of sphericity ($\varepsilon = 0.74$). Post-hoc *t*-tests for this analysis similarly indicated that functional connectivity (z') was highest in the ASD1 subgroup overall (Fig. 2D, Table 4). More specifically, connectivity between V1 and FP was increased in the ASD1 subgroup compared with the TD group, whereas it was atypically reduced in ASD2.

Correlations with Autism Symptomatology

In view of the distinct iFC patterns, correlational analyses were performed separately in the two ASD subgroups. In ASD1, we detected strong, positive correlations between distal connectivity, particularly for V1 and right FP, and two subdomains of the ADOS (Communication: $R^2(28) = 0.20$, $P = 0.013$; Repetitive and Restricted Behaviors: $R^2(28) = 0.23$, $P = 0.008$; Fig. 3A), indicating that increased iFC was associated with greater symptom severity.

Conversely, in the ASD2 subgroup, iFC between V1 and right FP was negatively correlated with multiple subdomains of the ADI-R (Communication: $R^2(20) = 0.27$, $P = 0.012$; Repetitive and Restricted Behaviors: $R^2(20) = 0.35$, $P = 0.004$; Fig. 3B). As functional connectivity in the ASD2 subgroup – which showed significantly weaker distal connectivity compared with the TD group – increased, autism symptom severity decreased. Symptomatology and KCC (*W*) values in V1 were not significantly correlated in either ASD subgroup.

Post-hoc Analyses with GSR

Results from ReHo analyses using GSR indicated a similar cluster of local overconnectivity in visual cortex, although this

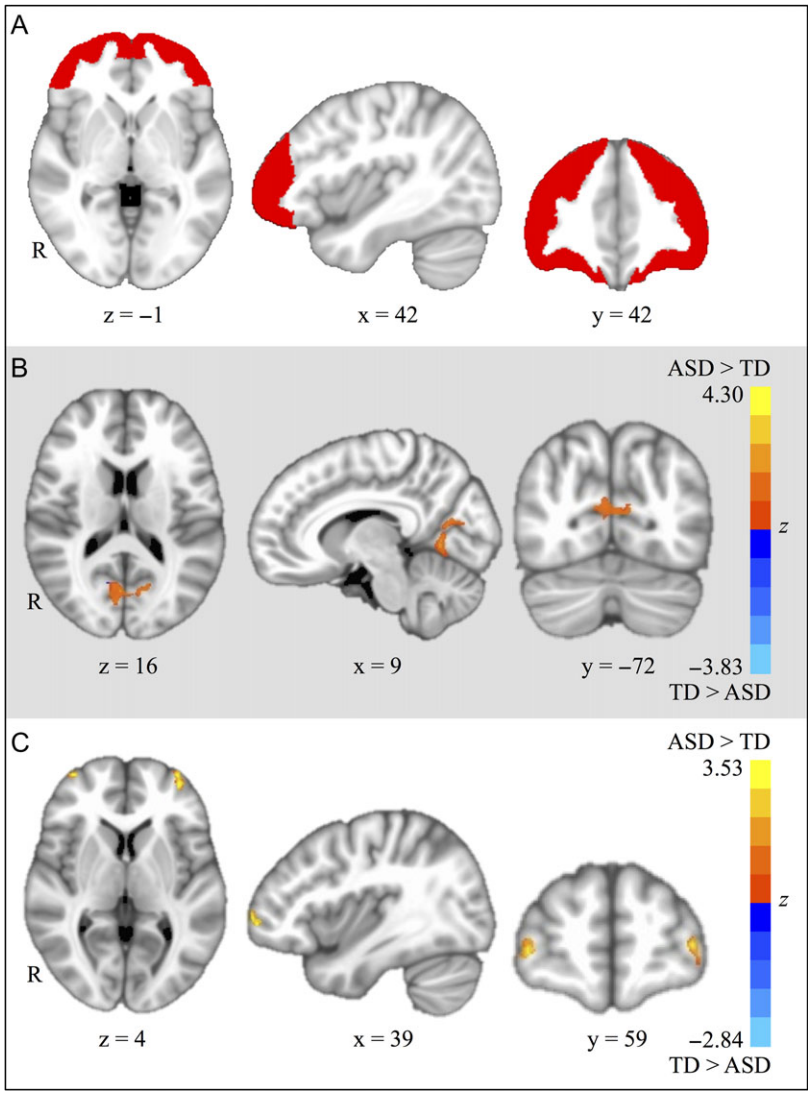

Figure 1. Regions-of-Interest (ROIs) and statistical parametric maps. (A) Left and right frontal pole (FP) ROIs from the Harvard-Oxford atlas. (B) Map of between-group differences (ASD > TD) in Regional Homogeneity (ReHo; P < 0.05, corrected). (C). Distal connectivity effects for V1 seed in left and right middle frontal gyri (MFG; P < 0.01, uncorrected). Data presented in radiological view; R = right.

Table 2 Clusters of between-group differences (ReHo: P < 0.05, corrected; ReHo seed to whole-brain: P < 0.01, uncorrected)

Cluster	Subregions	% of cluster vol.	Peak z	Vol. (voxels)	MNI peak coordinates		
					x	y	z
V1 (ReHo)	R calcarine gyrus	40.5	3.60	76	9	–72	16
	L calcarine gyrus	34.8					
	R lingual gyrus	22.4					
L MFG	L middle frontal gyrus	83.7	2.98	17	–37	55	4
	L middle orbital gyrus	4.5					
R MFG	R middle frontal gyrus	78.5	2.98	10	39	61	4
	R middle orbital gyrus	21.5					

between-group effect (ASD > TD), as well as the extent of the cluster, was reduced compared to ReHo analyses without GSR (Supplementary Fig. S3). Similar to previous findings (Qing et al. 2015), however, raw KCC (W) values were decreased with GSR in this region (Supplementary Fig. S4). Also in accordance with previous reports (Qing et al., 2015), spatial distributions of ReHo with and without GSR were largely similar (Supplementary Fig. S5–6). Importantly, the overall effects of distal connectivity still remained (i.e., overconnectivity between visual cortex and middle frontal gyrus; Supplementary Fig. S7).

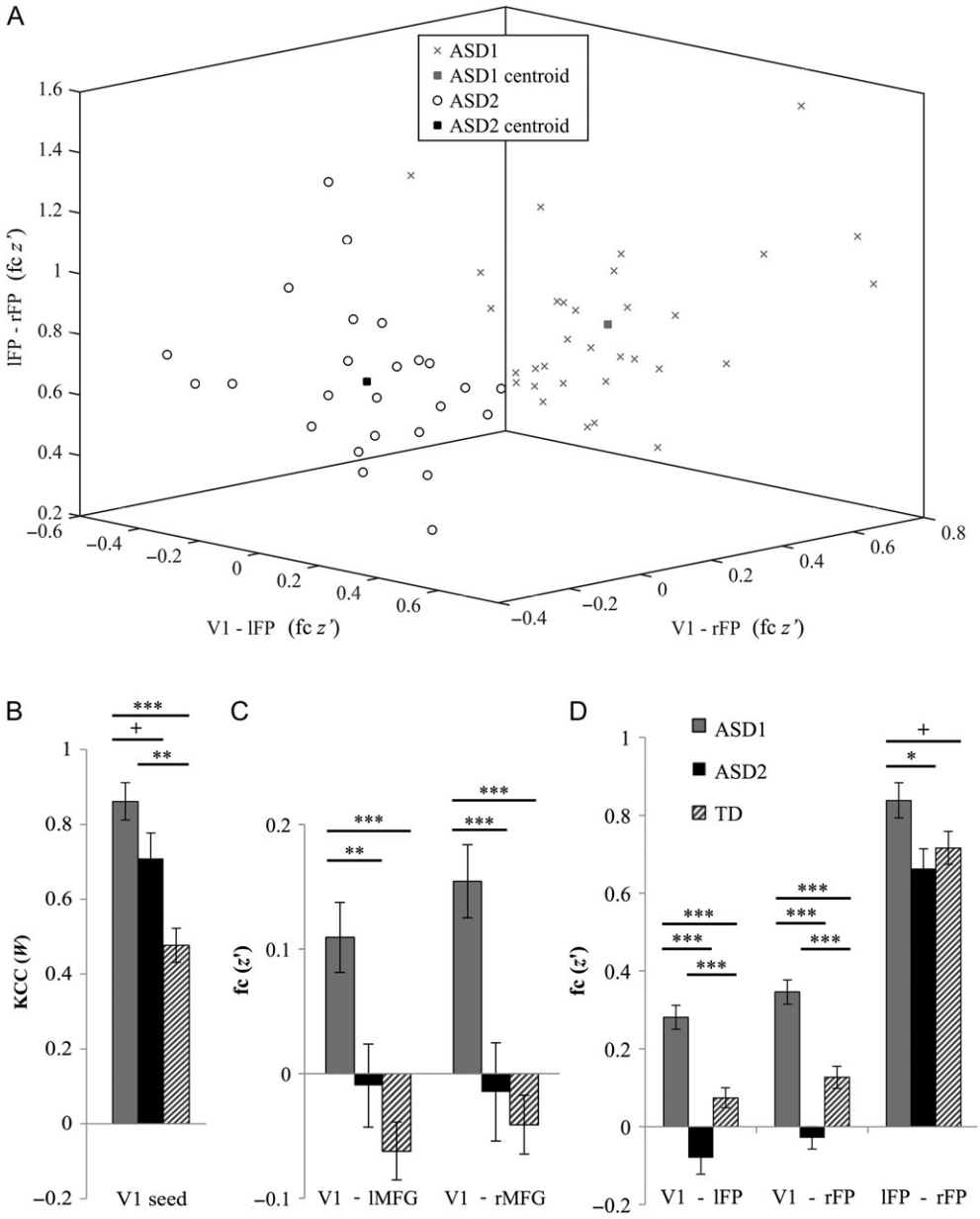

Figure 2. (*A*) Two ASD subgroups based on *k*-means clustering on functional connectivity (z') data: ASD1 (centroid: [0.281, 0.346, 0.838]) and ASD2 (centroid: [−0.080, −0.029, 00.663]), where centroid coordinates represent functional connectivity (z') between V1 and left FP, V1 and right FP, and left FP and right FP. (*B–D*) Group comparisons between the two ASD subgroups and TD group: (*B*) KCC (W) in the V1 seed from ReHo analyses; (*C*) Distal functional connectivity (z') between V1 and left and right middle frontal gyri (MFG); (*D*) Distal functional connectivity (z') between V1 and left and right FP, and interhemispheric functional connectivity (z') between left and right FP. See Table 4 for symbol denotations.

Discussion

While atypical iFC is often reported in ASDs, specific patterns of local and distal over- versus underconnectivity findings have been diverse and often inconsistent. In the current study, regional homogeneity (ReHo) was used to examine the links between local and distal connectivity in children and adolescents with ASDs compared with TD peers. We found local overconnectivity in ASDs in an occipital cluster with peak in primary visual cortex. For this posterior region, BOLD correlations with prefrontal regions were predominantly stronger in the ASD than in the TD group. However, two subgroups within our ASD cohort showed different connectivity patterns and behavioral correlations. One of them (ASD1) showed a robust pattern of occipital local overconnectivity and distal frontal overconnectivity, which was associated with autism symptom severity.

General Local Overconnectivity and Distal Underconnectivity? Doubly Wrong

According to the Belmonte hypothesis, atypically increased local connectivity is associated with reduced distal connectivity in autism (Belmonte et al. 2004). Early deviations in synaptic development may impact local cellular organization, as well as global, large-scale network structure (Uddin et al. 2010), and atypically increased synaptic connectivity on a local level may

Table 3 Demographic and diagnostic information for ASD subgroups

	ASD1 (n = 32)		ASD2 (n = 25)		Group comparison
	Mean (SD)	Range	Mean (SD)	Range	
Gender	6 female		4 female		$\chi^2(1) = 0.1$, P = 0.79
Handedness	7 left		2 left		$\chi^2(1) = 2.0$, P = 0.15
Age (years)	14.0 (2.4)	10.4–18.0	13.4 (2.9)	9.0–17.8	$t(55) = 0.9$, P = 0.38
Verbal IQ	102.3 (18.1)	73–147	101.7 (16.7)	70–131	$t(55) = 0.1$, P = 0.90
Non-verbal IQ	104.4 (19.6)	53–140	109.5 (17.6)	70–145	$t(55) = -1.0$, P = 0.32
Full-Scale IQ	103.6 (17.7)	66–141	105.4 (16.8)	73–139	$t(55) = -0.4$, P = 0.70
RMSD	0.07 (0.03)	0.02–0.11	0.06 (0.02)	0.03–0.11	$t(55) = 1.3$, P = 0.20
ADOS[a]					
Social interaction	7.2 (2.4)	2–12	8.2 (3.1)	3–14	$t(52) = -1.4$, P = 0.18
Communication	3.8 (2.3)	0–13	4.1 (1.9)	2–8	$t(52) = -0.6$, P = 0.55
Repetitive/Restricted	2.2 (1.4)	0–5	2.1 (1.6)	0–5	$t(52) = 0.2$, P = 0.84
ADI-R[b]					
Social interaction	17.7 (4.7)	7–28	19.2 (5.4)	6–28	$t(54) = -1.1$, P = 0.28
Communication	12.1 (4.4)	2–22	15.3 (5.2)	6–24	$t(54) = -2.4$, P = 0.02*
Repetitive behavior	6.3 (2.0)	2–12	5.7 (2.4)	1–11	$t(54) = 1.1$, P = 0.26
Psychotropic medication use	15 reported		12 reported		$\chi^2(1) = 0.01$, P = 0.93
Comorbidities (ADHD, depression, anxiety)	10 reported		9 reported		$\chi^2(1) = 0.14$, P = 0.71
Speech Onset Delay[c]					
Age of first words	18.4 (8.5) 9–36		28.6 (13.2) 10–50		$t(39) = 0.37$, P = 0.71
Age of first phrases	19.5 (9.7) 10–36		34.4 (12.0) 14–48		$t(39) = 1.41$, P = 0.17

[a]Subdomain data not available for 3 ASD2 participants.
[b]Subdomain data not available for 1 ASD2 participant.
*Indicates an uncorrected significance level of P < 0.05.
[c]Data in months obtained from ADI-R not available for 7 ASD1 participants and 9 ASD2 participants.

Table 4 Post-hoc statistical comparisons between groups

	t-Statistic	P-value	Signif. symbol
V1 KCC (W)			
ASD1 > ASD2	$t(55) = 1.85$	P = 0.070	+
ASD1 > TD	$t(81) = 5.48$	P < 0.001	***
ASD2 > TD	$t(74) = 2.88$	P = 0.005	**
V1 – Left middle frontal gyrus fc (z')			
ASD1 > ASD2	$t(55) = 2.74$	P = 0.008	**
ASD1 > TD	$t(81) = 4.66$	P < 0.001	***
ASD2 > TD	$t(74) = 1.30$	P = 0.198	n.s.
V1 – Right middle frontal gyrus fc (z')			
ASD1 > ASD2	$t(55) = 3.51$	P = 0.001	***
ASD1 > TD	$t(81) = 5.17$	P < 0.001	***
ASD2 > TD	$t(74) = 0.60$	P = 0.549	n.s.
V1 – Left frontal pole fc (z')			
ASD1 > ASD2	$t(55) = 7.13$	P < 0.001	***
ASD1 > TD	$t(81) = 5.14$	P < 0.001	***
ASD2 < TD	$t(74) = 3.32$	P = 0.001	***
V1 – Right frontal pole fc (z')			
ASD1 > ASD2	$t(55) = 8.66$	P < 0.001	***
ASD1 > TD	$t(81) = 5.02$	P < 0.001	***
ASD2 < TD	$t(74) = 3.42$	P = 0.001	***
Left frontal pole – Right frontal pole fc (z')			
ASD1 > ASD2	$t(55) = 2.58$	P = 0.013	*
ASD1 > TD	$t(81) = 1.90$	P = 0.061	+
ASD2 < TD	$t(74) = 0.75$	P = 0.456	n.s.

be paradoxically associated with reduced "computationally meaningful" connectivity between distal regions (Belmonte et al. 2004). While we did indeed observe local overconnectivity in our cohort of children and adolescents with ASDs, this effect was regionally specific and detected only in an occipital region (with peak in primary visual cortex). There was no evidence of *generalized* local overconnectivity (cf. Supplementary Fig. S5-6), in agreement with previous findings of regionally mixed

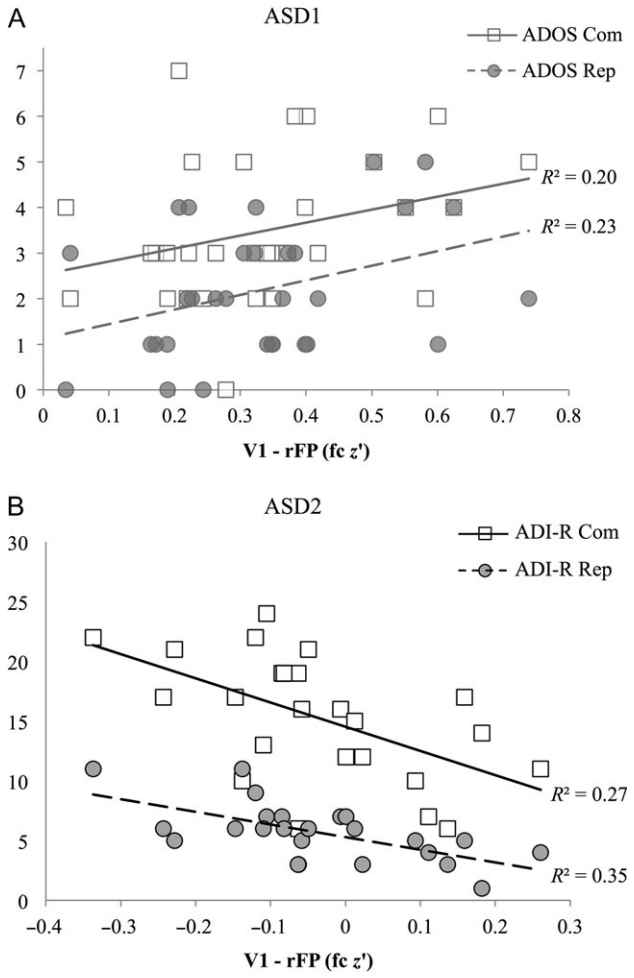

Figure 3. Correlations between distal (V1 – right FP) functional connectivity (z') and autism symptomatology in: (A) the ASD1 subgroup for ADOS; (B) the ASD2 subgroup for ADI-R.

patterns of local over- and underconnectivity in ASDs (Keown et al. 2013; Dajani and Uddin 2016; Nair et al. 2017), including findings generated without ReHo standardization (Maximo et al. 2013). Moreover, the locally overconnected occipital region predominantly showed distal frontal *overconnectivity*. In combination, these findings suggest that the theory of generalized local overconnectivity and long distance underconnectivity as a principle of atypical network organization in ASDs may be doubly wrong (cf. Picci et al. 2016).

Links Between "Early" Visual and Supramodal Prefrontal Cortex

Findings of robust local overconnectivity in primary visual cortex may relate to the special status of visual functioning in the neuropsychological profile of ASDs (Dakin and Frith 2005; Simmons et al. 2009). Evidence suggests that some perceptual abilities, especially in the visual modality, remain relatively spared in autism, with some potential islands of superior functioning (O'Riordan et al. 2001; Mottron et al. 2006; Eussen et al. 2016; Horlin et al. 2016). According to the "weak central coherence" model, however, visual processing is less directed in a "top-down" manner in autism (Frith 2003), and local processing biases may be at the expense of global processing (Happé 1996; Ropar and Mitchell 2002; Frith 2003; Happé and Frith 2006). Based on this model, overstimulated and underselective visual processing areas may dominate high-order cognitive processes, leading to impairments in integrating contextual information in complex perceptual and executive tasks (Belmonte et al. 2004). This may in turn relate to the frequent finding of atypically increased activity and connectivity of visual cortices (Kana et al. 2006; Simmons et al. 2009; Groen et al. 2010; Shen et al. 2012; Jao Keehn et al. 2016). A meta-analysis of fMRI studies examining a variety of visual processing tasks in autism reported overall higher task-related activity in occipital regions (Samson et al. 2012). Moreover, in studies examining interhemispheric communication, increased connectivity between visual regions (and weaker connectivity between frontal motor areas) across hemispheres was found in individuals with ASDs compared with TD individuals, suggesting intact interhemispheric transfer of visual information and enhanced perceptual processing (Barbeau et al. 2015; Clawson et al. 2015). This is consistent with current findings of the locally overconnected cluster in V1, which spans visual cortex bilaterally. Local overconnectivity in posterior regions has also been observed in ASDs in multiple rs-fMRI studies (Keown et al. 2013; Washington et al. 2013; Nair et al. 2017). Combined, these findings imply regionally specific abnormalities of local connectivity within visual cortex in autism, but do not provide insight regarding the links between local and distal iFC.

Our finding of predominant overconnectivity between (locally overconnected) visual cortex and distal prefrontal regions may appear inconsistent with the oft-cited hypothesis of fronto-posterior underconnectivity in ASDs (Just et al. 2012) and the hypothesis of early overgrowth in ASDs resulting in distal underconnectivity due to increased conduction delays (Lewis and Elman 2008). While the latter hypothesis is attractively mechanistic, many fcMRI studies supporting fronto-posterior underconnectivity tested task-driven BOLD correlations rather than iFC (cf. Müller et al. 2011), and such co-activation approaches have been shown to inflate underconnectivity findings in ASDs (Jones et al. 2010; Nair et al. 2014). A few previous resting state fcMRI studies have in fact reported fronto-posterior overconnectivity in ASDs (Supekar et al. 2013; Fishman et al. 2014; Abbott et al. 2016). Note that the present study did not show robustly significant occipito-frontal overconnectivity at the group-level. Instead, a predominance of higher means (i.e., slightly greater iFC) was found in the entire ASD group – an effect that was driven by a subgroup including just over half of the ASD participants (see below).

Functional Interpretation Requires Distinction of Autism Subtypes

Heterogeneity in ASDs, initially acknowledged based on behavioral observations (Happé et al. 2006), is highlighted by recent genetic findings suggesting that non-syndromic autism may encompass hundreds of disorders with differential causes and etiologies (Geschwind and State 2015; Vorstman et al. 2017). Although there may be convergence of etiological pathways (e.g., gene modules predominantly affecting synapses and circuit formation; Sahin and Sur 2015), it is likely that neurobiological diversity in ASDs persists into adolescence and beyond. This may be compounded by differences in early development of domain-general brain areas (e.g., perceptual cortex vs. language regions) in individuals with and without speech onset delays (for a review, see Mottron et al. (2014)), as well as in life experience (e.g., treatment history) that further add to

variability within the ASD population. Tests for group-level differences between TD and ASD cohorts may therefore only detect atypical neurofunctional patterns that are shared across ASD variants. These may be common, but small, denominators that are only modestly informative of crucial patterns of brain anomalies in any given individual within the cohort. Testing ASD samples for clusters (subgroups) of participants characterized by shared neural features of interest is crucial to overcome the limitations of group-level analyses.

We indeed identified two subgroups of ASD participants that were distinctly differentiated by their occipito-frontal iFC patterns. Interestingly, these two subgroups were similar with regard to demographic and diagnostic measures, and comorbidities. Connectivity differences were also not explained by psychotropic medication use (despite recent findings reported by Linke et al. (2017)). In one ASD subgroup (ASD1), very high levels of local connectivity in visual cortex were accompanied by abnormally strong distal iFC with bilateral prefrontal regions. In this subgroup, this pattern of local to distal overconnectivity was associated with greater symptom severity. Conversely, in a second subgroup (ASD2), local overconnectivity in primary visual cortex was associated with more typical patterns of overall weak distal iFC with prefrontal regions. This group displayed inverse links with diagnostic measures (i.e., *lower* occipito-frontal iFC was associated with greater symptom severity).

The pattern across both ASD subgroups suggests that divergence from neurotypical patterns at both extremes may be linked to more severe symptomatology. However, both connectivity patterns and brain–behavior relationships were distinct and largely opposite in the two ASD subgroups. This does not imply a claim that our analyses may have identified two ASD subtypes. *K*-means clustering was based only on a few iFC features, whereas the number of neural features needed to identify a broader catalog of ASD subtypes will presumably be very large. Nevertheless, the stark iFC differences accompanied by opposing brain–behavior links suggests that the two ASD subgroups capture a small aspect of neurobiological variability within the population.

The two subgroups also differed in their connectivity between visual cortex and MFG bilaterally (i.e., the regions found to be maximally overconnected at the whole-group level with the occipital site of local overconnectivity). In the TD group, iFC between visual cortex and the smaller ROI in task-positive dorsolateral prefrontal cortex was negative. In typical development, such anticorrelations are thought to indicate a division of labor between functionally specialized networks (here: visual and executive; Fransson 2006) and to reflect network segregation, with activity being correlated within, but anticorrelated across networks (Greicius et al. 2003; Fox et al. 2005; Easson et al. 2017). Our findings suggest that neurotypical segregation between visual and executive regions was severely affected – and in fact reversed – in the ASD1 subgroup (which showed instead positive BOLD correlations), whereas it appeared only weakened in the other ASD subgroup. However, note that in ASD2, anticorrelations between V1 and prefrontal regions overall were associated with *more severe* symptomatology, suggesting that in this subgroup, brain–behavior links also differed from neurotypical.

Limitations

Several limitations are worth noting. As BOLD ReHo examines local connectivity at a macroscopic level with relatively modest spatial resolution, it may not relate straightforwardly to microscopic findings at the cellular level. It would therefore be speculative to link our results to postmortem evidence of minicolumnar anomalies with reduced lateral inhibition (Casanova et al. 2003; Casanova and Trippe 2009) or to the more general model of increased excitation/inhibition ratios in ASDs (Rubenstein and Merzenich 2003; Nelson and Valakh 2015).

Methodological differences related to eye status must also be considered. Our local overconnectivity finding in occipital lobe during eyes-open rs-fMRI scans contrasts with a large sample study by Di Martino et al. (2014). However, the inclusion of resting-state data from participants with eyes closed in this latter study was recently shown by Nair et al. (2017) to heavily impact regional homogeneity patterns, particularly in the occipital lobe (see also Yang et al. 2007; McAvoy et al. 2008; Xu et al. 2014). Local occipital overconnectivity in eyes-open states has indeed been found in several independent ASD cohorts (Washington et al. 2013; Nair et al. 2017).

Conclusions

Contrary to a popular hypothesis, ASDs are not associated with general local overconnectivity accompanied by distal underconnectivity. Instead, we found local overconnectivity to be regionally specific and robust only in and around primary visual cortex. This site showed predominantly increased distal iFC with bilateral prefrontal regions, compared with a TD group. The effect was only pronounced in a subgroup of ASD participants, where it was associated with greater symptom severity; inverse symptom correlations were seen in a second ASD subgroup. Findings suggest that simple generalizing accounts of connectivity anomalies cannot capture nuanced and regionally specific patterns in ASDs, and that group-level analyses do not adequately reflect the neurofunctional heterogeneity within the ASD population.

Supplementary Material

Supplementary material is available at *Cerebral Cortex* online.

Funding

This work was supported by the National Institutes of Health (R01-MH081023 and R01-MH101173 to R.A.M.; K01-MH097972 to I.F.); an Autism Science Foundation Undergraduate Summer Research Award (E.P.); a San Diego State University Summer Undergraduate Research Award (E.P.); and support from the National Institutes of Health Initiative for Maximizing Student Development (IMSD) Program (R25GM058906 to E.P.), with additional funding for MRI scanning in eight participants from the Congressionally Directed Medical Research Programs (AR093335 to J. Pineda).

Notes

Special thanks are extended to the children and families who participated. *Conflict of Interest*: None declared.

References

Abbott AE, Nair A, Keown CL, Datko M, Jahedi A, Fishman I, Müller R-A. 2016. Patterns of atypical functional connectivity and behavioral links in autism differ between default, salience, and executive networks. Cereb Cortex. 26:4034–4045.

American Psychiatric Association. 2000. Diagnostic and statistical manual of mental disorders – IV – TR. 4th ed. Washington, DC: American Psychiatric Association.

American Psychiatric Association. 2013. Diagnostic and statistical manual of mental disorders – V. 4th ed. Washington, DC: American Psychiatric Association.

Barbeau EB, Lewis JD, Doyon J, Benali H, Zeffiro TA, Mottron L. 2015. A greater involvement of posterior brain areas in interhemispheric transfer in autism: fMRI, DWI and behavioral evidences. Neuroimage. 8:267–280.

Belmonte MK, Allen G, Beckel-Mitchener A, Boulanger LM, Carper RA, Webb SJ. 2004. Autism and abnormal development of brain connectivity. J Neurosci. 24:9228–9231.

Birn RM. 2007. The behavioral significance of spontaneous fluctuations in brain activity. Neuron. 56:8–9.

Buckner RL, Krienen FM, Yeo BT. 2013. Opportunities and limitations of intrinsic functional connectivity MRI. Nat Neurosci. 16:832–837.

Casanova MF, Buxhoeveden D, Gomez J. 2003. Disruption in the inhibitory architecture of the cell minicolumn: implications for autisim. Neuroscientist. 9:496–507.

Casanova M, Trippe J. 2009. Radial cytoarchitecture and patterns of cortical connectivity in autism. Philos Trans R Soc Lond B Biol Sci. 364:1433–1436.

CDC. 2015. Estimated prevalence of autism and other developmental disabilities following questionnaire changes in the 2014 National Health Interview Survey. Natl Health Stat Report. 87:1–20.

Clawson A, Clayson PE, South M, Bigler ED, Larson MJ. 2015. An electrophysiological investigation of interhemispheric transfer time in children and adolescents with high-functioning autism spectrum disorders. J Autism Dev Disord. 45:363–375.

Cordes D, Haughton VM, Arfanakis K, Carew JD, Turski PA, Moritz CH, Quigley MA, Meyerand ME. 2001. Frequencies contributing to functional connectivity in the cerebral cortex in "resting-state" data. AJNR Am J Neuroradiol. 22:1326–1333.

Cox RW. 1996. AFNI: software for analysis and visualization of functional magnetic resonance neuroimages. Comput Biomed Res. 29:162–173.

Cox RW, Chen G, Glen DR, Reynolds RC, Taylor PA. 2017. fMRI clustering and false-positive rates. Proc Natl Acad Sci USA. 114:E3370–E3371.

Dajani DR, Uddin LQ. 2016. Local brain connectivity across development in autism spectrum disorder: a cross-sectional investigation. Autism Res. 9:43–54.

Dakin S, Frith U. 2005. Vagaries of visual perception in autism. Neuron. 48:497–507.

Damasio AR, Maurer RG. 1978. A neurological model for childhood autism. Arch Neurol. 35:777–786.

Desikan RS, Ségonne F, Fischl B, Quinn BT, Dickerson BC, Blacker D, Buckner RL, Dale AM, Maguire RP, Hyman BT, et al. 2006. An automated labeling system for subdividing the human cerebral cortex on MRI scans into gyral based regions of interest. Neuroimage. 31:968–980.

Di Martino A, Yan CG, Li Q, Denio E, Castellanos FX, Alaerts K, Anderson JS, Assaf M, Bookheimer SY, Dapretto M, et al. 2014. The autism brain imaging data exchange: towards a large-scale evaluation of the intrinsic brain architecture in autism. Mol Psychiatry. 19:659–667.

Easson AK, Fatima Z, McIntosh AR. 2017. Defining subtypes of autism spectrum disorder using static and dynamic functional connectivity. bioRxiv.

Eklund A, Nichols TE, Knutsson H. 2016. Cluster failure: why fMRI inferences for spatial extent have inflated false-positive rates. Proc Natl Acad Sci USA. 113:201602413.

Eussen ML, Gool AR, Louwerse A, Verhulst FC, Greaves-Lord K. 2016. Superior disembedding performance in childhood predicts adolescent severity of repetitive behaviors: a seven years follow-up of individuals with autism spectrum disorder. Autism Res. 9:282–291.

Fishman I, Keown CL, Lincoln AJ, Pineda JA, Müller R-A. 2014. Atypical cross talk between mentalizing and mirror neuron networks in autism spectrum disorder. JAMA Psychiatry. 71:751–760.

Fox MD, Snyder AZ, Vincent JL, Corbetta M, Van Essen DC, Raichle ME. 2005. The human brain is intrinsically organized into dynamic, anticorrelated functional networks. Proc Natl Acad Sci USA. 102:9673–9678.

Fox MD, Zhang D, Snyder AZ, Raichle ME. 2009. The global signal and observed anticorrelated resting state brain networks. J Neurophysiol. 101:3270–3283.

Fransson P. 2006. How default is the default mode of brain function? Further evidence from intrinsic BOLD signal fluctuations. Neuropsychologia. 44:2836–2845.

Frith U. 2003. Autism: explaining the enigma. 2nd ed. Malden, MA: Wiley-Blackwell.

Geschwind DH, State MW. 2015. Gene hunting in autism spectrum disorder: on the path to precision medicine. Lancet Neurol. 14:1109–1120.

Gotts SJ, Saad ZS, Jo HJ, Wallace GL, Cox RW, Martin A. 2013. The perils of global signal regression for group comparisons: a case study of Autism Spectrum Disorders. Front Hum Neurosci. 7:356.

Greicius MD, Krasnow B, Reiss AL, Menon V. 2003. Functional connectivity in the resting brain: a network analysis of the default mode hypothesis. Proc Natl Acad Sci USA. 100:253–258.

Groen WB, Tesink C, Petersson KM, van Berkum J, van der Gaag RJ, Hagoort P, Buitelaar JK. 2010. Semantic, factual, and social language comprehension in adolescents with autism: an FMRI study. Cereb Cortex. 20:1937–1945.

Happé FGE. 1996. Studying weak central coherence at low levels: children with autism do not succumb to visual illusions. A research note. J Child Psychol Psychiatry. 37:873–877.

Happé F, Frith U. 2006. The weak coherence account: detail-focused cognitive style in autism spectrum disorders. J Autism Dev Disord. 36:5–25.

Happé F, Ronald A, Plomin R. 2006. Time to give up on a single explanation for autism. Nat Neurosci. 9:1218–1220.

Horlin C, Black M, Falkmer M, Falkmer T. 2016. Proficiency of individuals with autism spectrum disorder at disembedding figures: a systematic review. Dev Neurorehabil. 19:54–63.

Itahashi T, Yamada T, Watanabe H, Nakamura M, Ohta H, Kanai C, Iwanami A, Kato N, Hashimoto R. 2015. Alterations of local spontaneous brain activity and connectivity in adults with high-functioning autism spectrum disorder. Mol Autism. 6:30.

Jao Keehn RJ, Sanchez SS, Stewart CR, Zhao W, Grenesko-Stevens EL, Keehn B, Müller R-A. 2016. Impaired downregulation of visual cortex during auditory processing is associated with autism symptomatology in children and adolescents with autism spectrum disorder. Autism Res. 10:130–143.

Jenkinson M, Smith S. 2001. A global optimisation method for robust affine registration of brain images. Med Image Anal. 5:143–156.

Jiang L, Hou XH, Yang N, Yang Z, Zuo XN. 2015. Examination of local functional homogeneity in autism. Biomed Res Int. 2015:174371.

Johnson MH. 2011. Interactive specialization: a domain-general framework for human functional brain development. Dev Cogn Neurosci. 1:7–21.

Jones TB, Bandettini PA, Kenworthy L, Case LK, Milleville SC, Martin A, Birn RM. 2010. Sources of group differences in functional connectivity: an investigation applied to autism spectrum disorder. Neuroimage. 49:401–414.

Just MA, Keller TA, Malave VL, Kana RK, Varma S. 2012. Autism as a neural systems disorder: a theory of frontal-posterior underconnectivity. Neurosci Biobehav Rev. 36:1292–1313.

Kana RK, Keller TA, Cherkassky VL, Minshew NJ, Just MA. 2006. Sentence comprehension in autism: thinking in pictures with decreased functional connectivity. Brain. 129:2484–2493.

Keller CJ, Bickel S, Honey CJ, Groppe DM, Entz L, Craddock RC, Lado FA, Kelly C, Milham M, Mehta AD. 2013. Neurophysiological investigation of spontaneous correlated and anticorrelated fluctuations of the BOLD signal. J Neurosci. 33:6333–6342.

Kendall M, Gibbsons JD. 1990. Rank correlation methods. Oxford: Oxford University Press.

Keown C, Shih P, Nair A, Peterson N, Mulvey M, Müller RA. 2013. Local functional overconnectivity in posterior brain regions is associated with symptom severity in autism spectrum disorders. Cell Rep. 5:567–572.

Lewis JD, Elman JL. 2008. Growth-related neural reorganization and the autism phenotype: a test of the hypothesis that altered brain growth leads to altered connectivity. Dev Sci. 11:135–155.

Linke AC, Olson L, Gao Y, Fishman I, Müller R-A. 2017. Psychotropic medication use in autism spectrum disorders may affect functional brain connectivity. Biol Psychiatry Cogn Neurosci Neuroimaging. 2:518–527.

Lord C, Risi S, Lambrecht L, Cook EH, Leventhal BL, DiLavore PC, Pickles A, Rutter M. 2000. The autism diagnostic observation schedule—generic: a standard measure of social and communication deficits associated with the spectrum of autism. J Autism Dev Disord. 30:205–223.

Lord C, Rutter M, Le Couteur A. 1994. Autism diagnostic interview-revised: a revised version of a diagnostic interview for caregivers of individuals with possible pervasive developmental disorders. J Autism Dev Disord. 24:659–685.

Maximo JO, Cadena EJ, Kana RK. 2014. The implications of brain connectivity in the neuropsychology of autism. Neuropsychol Rev. 24:16–31.

Maximo JO, Keown CL, Nair A, Müller R-A. 2013. Approaches to local connectivity in autism using resting state functional connectivity MRI. Front Hum Neurosci. 7:605.

McAvoy M, Larson-Prior L, Nolan TS, Vaishnavi SN, Raichle ME, d'Avossa G. 2008. Resting states affect spontaneous BOLD oscillations in sensory and paralimbic cortex. J Neurophysiol. 100:922–931.

Menon V. 2011. Large-scale brain networks and psychopathology: a unifying triple network model. Trends Cogn Sci. 15: 483–506.

Minshew NJ, Williams DL. 2007. The new neurobiology of autism: cortex, connectivity, and neuronal organization. Arch Neurol. 64:945–950.

Mottron L, Belleville S, Rouleau GA, Collignon O. 2014. Linking neocortical, cognitive, and genetic variability in autism with alterations of brain plasticity: the Trigger-Threshold-Target model. Neurosci Biobehav Rev. 47:735–752.

Mottron L, Dawson M, Soulieres I, Hubert B, Burack J. 2006. Enhanced perceptual functioning in autism: an update, and eight principles of autistic perception. J Autism Dev Disord. 36:27–43.

Müller RA, Shih P, Keehn B, Deyoe JR, Leyden KM, Shukla DK. 2011. Underconnected, but how? A survey of functional connectivity MRI studies in autism spectrum disorders. Cereb Cortex. 21:2233–2243.

Nair S, Jao Keehn RJ, Berkebile MM, Maximo JO, Witkowska N, Müller R-A. 2017. Local resting state functional connectivity in autism: site and cohort variability and the effect of eye status. Brain Imaging Behav. 12:168–179.

Nair A, Keown CL, Datko M, Shih P, Keehn B, Müller RA. 2014. Impact of methodological variables on functional connectivity findings in autism spectrum disorders. Hum Brain Mapp. 35:4035–4048.

Nebel MB, Joel SE, Muschelli J, Barber AD, Caffo BS, Pekar JJ, Mostofsky SH. 2014. Disruption of functional organization within the primary motor cortex in children with autism. Hum Brain Mapp. 35:567–580.

Nelson SB, Valakh V. 2015. Excitatory/inhibitory balance and circuit homeostasis in autism spectrum disorders. Neuron. 87:684–698.

Oldfield RC. 1971. The assessment and analysis of handedness: the Edinburgh Inventory. Neuropsychologia. 9:97–113.

O'Riordan MA, Plaisted KC, Driver J, Baron-Cohen S. 2001. Superior visual search in autism. J Exp Psychol Hum Percept Perform. 27:719–730.

Paakki JJ, RahkoJ, LongX, MoilanenI, TervonenO, NikkinenJ, StarckT, RemesJ, HurtigT, HaapsamoH, et al. 2010. Alterations in regional homogeneity of resting-state brain activity in autism spectrum disordersBrain Res. 1321: 169–179.

Picci G, Gotts SJ, Scherf KS. 2016. A theoretical rut: revisiting and critically evaluating the generalized under/over-connectivity hypothesis of autism. Dev Sci. 19:524–549.

Power JD, Barnes KA, Snyder AZ, Schlaggar BL, Petersen SE. 2012. Spurious but systematic correlations in functional connectivity MRI networks arise from subject motion. Neuroimage. 59:2142–2154.

Power JD, Mitra A, Laumann TO, Snyder AZ, Schlaggar BL, Petersen SE. 2014. Methods to detect, characterize, and remove motion artifact in resting state fMRI. Neuroimage. 84:320–341.

Power JD, Schlaggar BL, Petersen SE. 2015. Recent progress and outstanding issues in motion correction in resting state fMRI. Neuroimage. 105C:536–551.

Qing Z, Dong Z, Li S, Zang Y, Liu D. 2015. Global signal regression has complex effects on regional homogeneity of resting state fMRI signal. Magn Reson Imaging. 33:1306–1313.

Ropar D, Mitchell P. 2002. Shape constancy in autism: the role of prior knowledge and perspective cues. J Child Psychol Psychiatry. 43:647–653.

Rubenstein JL, Merzenich MM. 2003. Model of autism: increased ratio of excitation/inhibition in key neural systems. Genes Brain Behav. 2:255–267.

Sahin M, Sur M. 2015. Genes, circuits, and precision therapies for autism and related neurodevelopmental disorders. Science. 350 (6263). pii: aab3897. doi: 10.1126/science.aab3897.

Samson F, Mottron L, Soulieres I, Zeffiro TA. 2012. Enhanced visual functioning in autism: an ALE meta-analysis. Hum Brain Mapp. 33:1553–1581.

Schölvinck ML, Maier A, Ye FQ, Duyn JH, Leopold DA. 2010. Neural basis of global resting-state fMRI activity. Proc Natl Acad Sci USA. 107:10238–10243.

Shen MD, Shih P, Ottl B, Keehn B, Leyden KM, Gaffrey MS, Muller RA. 2012. Atypical lexicosemantic function of extrastriate cortex in autism spectrum disorder: evidence from functional and effective connectivity. Neuroimage. 62: 1780–1791.

Shih P, Keehn B, Oram JK, Leyden KM, Keown CL, Müller R-A. 2011. Functional differentiation of posterior superior

temporal sulcus in autism: a functional connectivity magnetic resonance imaging study. Biol Psychiatry. 70:270–277.
Shukla DK, Keehn BM, Müller R-A. 2010. Regional homogeneity of fMRI time series in autism spectrum disorders. Neurosci Lett. 476:46–51.
Simmons DR, Robertson AE, McKay LS, Toal E, McAleer P, Pollick FE. 2009. Vision in autism spectrum disorders. Vision Res. 49:2705–2739.
Smith SM, Jenkinson M, Woolrich MW, Beckmann CF, Behrens TEJ, Johansen-Berg H, Bannister PR, De Luca M, Drobnjak I, Flitney DE, et al. 2004. Advances in functional and structural MR image analysis and implementation as FSL, Neuroimage 23(Suppl 1):S208–S219.
Sporns O. 2013. Network attributes for segregation and integration in the human brain. Curr Opin Neurobiol. 23:162–171.
Supekar K, Uddin LQ, Khouzam A, Phillips J, Gaillard WD, Kenworthy LE, Yerys BE, Vaidya CJ, Menon V. 2013. Brain hyperconnectivity in children with autism and its links to social deficits. Cell Rep. 5:738–747.
Uddin LQ, Supekar K, Menon V. 2010. Typical and atypical development of functional human brain networks: insights from resting-state FMRI. Front Syst Neurosci. 4:21.
Van Dijk KR, Hedden T, Venkataraman A, Evans KC, Lazar SW, Buckner RL. 2010. Intrinsic functional connectivity as a tool for human connectomics: theory, properties, and optimization. J Neurophysiol. 103:297–321.
van Dijk KRA, Sabuncu MR, Buckner RL. 2012. The influence of head motion on intrinsic functional connectivity MRI. Neuroimage. 59:431–438.
Vissers ME, Cohen MX, Geurts HM. 2012. Brain connectivity and high functioning autism: a promising path of research that needs refined models, methodological convergence, and stronger behavioral links. Neurosci Biobehav Rev. 36:604–625.
Vorstman JAS, Parr JR, Moreno-De-Luca D, Anney RJL, Nurnberger JI Jr, Hallmayer JF. 2017. Autism genetics: opportunities and challenges for clinical translation. Nat Rev Genet. 18:362.
Washington SD, Gordon EM, Brar J, Warburton S, Sawyer AT, Wolfe A, Mease-Ference ER, Girton L, Hailu A, Mbwana J, et al. 2013 Dysmaturation of the default mode network in autism. Hum Brain Mapp. 35:1284–1296.
Wass S. 2011. Distortions and disconnections: disrupted brain connectivity in autism. Brain Cogn. 75:18–28.
Wechsler D. 1999. Wechsler Abbreviated Scale of Intelligence (WASI). San Antonio, Texas: Psychological Corporation.
Williams EL, Casanova MF. 2010. Autism and dyslexia: a spectrum of cognitive styles as defined by minicolumnar morphometry. Med Hypotheses. 74:59–62.
Xu P, Huang R, Wang J, Van Dam NT, Xie T, Dong Z, Chen C, Gu R, Zang Y-F, He Y, et al. 2014. Different topological organization of human brain functional networks with eyes open versus eyes closed. Neuroimage. 90:246–255.
Yang H, Long X-Y, Yang Y, Yan H, Zhu C-Z, Zhou X-P, Zang Y-F, Gong Q-Y. 2007. Amplitude of low frequency fluctuation within visual areas revealed by resting-state functional MRI. Neuroimage. 36:144–152.
Zang Y, Jiang T, Lu Y, He Y, Tian L. 2004. Regional homogeneity approach to fMRI data analysis. Neuroimage. 22:394–400.
Zhang Y, Brady M, Smith S. 2001. Segmentation of brain MR images through a hidden Markov random field model and the expectation-maximization algorithm. IEEE Trans Med Imaging. 20:45–57.